J. Membrane Biol. 15, 87–106 (1974)

Computer Simulation of Na* Wash-out Kinetics in Frog Skin Epidermis

Ernst G. Huf and John R. Howell

Departments of Physiology and Biometry, Virginia Commonwealth University, Richmond, Virginia 23219

Received 26 February 1973; revised 22 May 1973

Summary. The multicompartmental frog skin epidermis model proposed in a previous paper was applied to computer simulation studies on the kinetics of the wash-out process of Na* from frog skin. Both the kinetics of loading of the model membrane with Na* from the outside to reach steady-state conditions in all internal compartments, and of the wash-out process were followed. This was done for the case when two Na^+ pumps were operative, or inoperative, simulating the inhibitory effect of ouabain on active Na^+ transport in frog skin. The two pumps were characterized as transmembrane Na^+ flow pumps, and internal Na^+ maintenance pumps which contribute but little to net inward Na^+ flux. The simulation results were in good agreement, both qualitatively and quantitatively, with data in the literature on the behavior of frog skin epidermis. This analysis gives support especially to the views held by Zerahn on location and size of the active Na^+ transport pool in skin epithelium. Beyond this, however, this study clearly delineates the experimental conditions under which the estimation of the Na^+ transport pool by the method of measuring the wash-out rate of Na* may be successful, and under which conditions this method will fail.

Of the investigations on the kinetics of wash-out of Na* from frog skin epidermis with intent to obtain a better understanding of the compartments involved in flow of Na^+ across this epithelial membrane, the studies by Zerahn [12] are remarkable for three reasons. 1) He showed "within the limitations of the method used that the Na* pool behaves as if it has passed the transport mechanism ...". 2) All "attempts to find conditions where a transport pool could be demonstrated have been in vain". 3) He was led to conclude "that the mechanism for active transport of sodium is effective at the outer surface of the frog skin."

We were able to fully confirm these conclusions by computer simulation of the rates of Na* wash-out, applied to the multicompartmental epidermis model proposed and studied in considerable detail in a previous paper [7]. The good agreements in facts obtained from actual laboratory experiments

and from computer simulation studies, both those presented earlier [7] as well as those presented here, suggest that the design and function of the epidermis model on which this study is based bears close resemblance to the structure and function of frog skin epidermis. From the results of studies on the kinetic behavior of the model, the inference may be drawn that success, or failure to obtain from wash-out experiments on frog skin a value for a pool of Na^+ awaiting transport depends, very critically, on the observance of certain timing conditions, as will be pointed out.

1. Model and Parameters

This study is based on the model 10E described in a previous publication [7]. The compartments and their connections are shown in Fig. 1 of that paper. The assumptions made are as follows: Pathways $1 \rightleftarrows 2$ and $1 \rightleftarrows 3$ are the pathways which Na^+ takes from the outside fluid chamber compartment (1) via the cornified layer into the subcorneal space (2), and via the cornified layer and cell junctions into the first reacting cell layers, 1.RCL(3). These are considered to be passive processes. Na^+ also moves passively into the 1.RCL from the subcorneal space across what may be a Na^+ permselective barrier. From the 1.RCL(3) Na^+ moves passively via cell junctions into all the remaining epithelial cells (4). "Strong" Na^+ pumps are assumed to operate between 3 and 5; i.e., Na^+ is pumped out of the 1.RCL into the extracellular space (5). This is thought to be the main transepithelial active Na^+ transporting mechanism. "Weak" Na^+ pumps, contributing little to transepithelial active Na^+ transport, are assumed to operate between the remaining epithelial cells (4) and the extracellular space (5). From 5, Na^+ diffuses across the basement membrane into the inside chamber fluid compartment (7). In the present work it is assumed that the "slowly exchangeable" Na^+ compartment in epidermis (6) is not involved. Flows between the subcorneal space (2) and the extracellular space (5) via the inner set of epidermal tight cell junctions, for the present, has been assumed to be negligible. The compartmental volumes used are given in the legend of Fig. 1 of ref. [7]. This model is in agreement with essential components of the histological structure of the epidermis. The rate constants (min^{-1}) for 10E are as follows: $k_{12} = 16 \times 10^{-5}$; $k_{21} = 8$; $k_{13} = 2 \times 10^{-5}$; $k_{31} = 0.2$; $k_{23} = 1.0$; $k_{32} = 0.2$; $k_{34} = 4 \times 10^{-2}$; $k_{43} = 5 \times 10^{-3}$; $k_{35} = 10$; $k_{53} = 0.1$; $k_{45} = 0.5$; $k_{54} = 2.0$; $k_{57} = 4$; $k_{75} = 4 \times 10^{-4}$; $k_{46} = 0$; $k_{64} = 0$. As has been mentioned above, two Na^+ pumps are assumed to operate, a "strong" pump between $3 \rightarrow 5$, and a "weak" pump between

$4 \rightarrow 5$ [7, 11]. These assumptions are quantitatively expressed by the disproportion in the ratios k_{35}/k_{53}, and k_{45}/k_{54}; they are not chosen inversely proportional to the respective compartmental volumes involved, as should be the case for simple passive diffusion according to Fick's law: $k = P \cdot A/V$, where P is the apparent permeability coefficient, A is the area involved and V is the volume of the compartment from which Na^+ moves. The rate constants are taken as time independent, and all volumes are assumed to remain constant, a restriction which we intend to remove later to simulate other than Na^+ wash-out observations made of skin epithelium. Besides 10E we have studied the behavior of a few other models having the same design as Fig. 1 in ref. [7] but which differed in certain k-values. These changes will be presented in the appropriate sections of the text.

2. Flow Equations and Solutions

Excluding compartment 6, the matrix of differential flow equations is as follows:

$$\begin{bmatrix} \dot{S}_1 \\ \dot{S}_2 \\ \dot{S}_3 \\ \dot{S}_4 \\ \dot{S}_5 \\ \dot{S}_7 \end{bmatrix} = \begin{bmatrix} -k_1 & k_{21} & k_{31} & 0 & 0 & 0 \\ k_{12} & -k_2 & k_{32} & 0 & 0 & 0 \\ k_{13} & k_{23} & -k_3 & k_{43} & k_{53} & 0 \\ 0 & 0 & k_{34} & -k_4 & k_{54} & 0 \\ 0 & 0 & k_{35} & k_{45} & -k_5 & k_{75} \\ 0 & 0 & 0 & 0 & k_{57} & -k_7 \end{bmatrix} \begin{bmatrix} S_1 \\ S_2 \\ S_3 \\ S_4 \\ S_5 \\ S_7 \end{bmatrix}$$

where $\dot{S} = dS/dt$, and $-k_1 = -(k_{12} + k_{13})$; $-k_2 = -(k_{21} + k_{23})$; $-k_3 = -(k_{31} + k_{32} + k_{34} + k_{35})$; $-k_4 = -(k_{43} + k_{45})$; $-k_5 = -(k_{53} + k_{54} = k_{57})$; $-k_7 = -k_{75}$. S_j is the amount of sodium in compartment j ($j = 1, 2, 3, 4, 5, 7$). Depending on what we were aiming at, a value of $S_j = 1$ is taken to mean 1 μEquiv Na^+; or a value of $S_j^* = 1$ is taken as 1×10^8 cpm Na*.

The six simultaneous differential equations (which can readily be rewritten in the more conventional way) were solved for values of S_j by computer programming, using an IBM 360 computer with application of the Continuous System Modeling Program (CSMP). The integration interval was 0.02 min. Print-out data were obtained for 30 min at 0.5-min intervals for the data presented in Section 6*a*, and 0.2-min intervals for the data presented in Sections 6*b*, *c*, *d*.

3. Initial Conditions

In some of the studies we were interested in the kinetics of influx, backflux (outflux) and net flow of Na^+ across the model membrane to reach steady states, with changes in the Na^+ pump rate coefficients. The initial con-

ditions, here, were for influx: $S_1 = 575$, all other compartments empty at zero time; for backflux: $S_7 = 575$, all other compartments empty at zero time; for net flux: $S_1 = S_7 = 575$, all other compartments empty at zero time.

In other studies we were interested in bringing the model membrane 10E, already considered in Na^+ steady state with respect to $S_1 = S_7 = 575$, into Na* steady state, and then observed the rates of Na* wash-out (decay) in all compartments. The initial condition was $S_1^* = 575 \times 10^8$, all other compartments free of Na* at zero time.

4. Conditions for Na* Wash-out

For the "loading phase" of 10E using Na*, all k coefficients specified for this model in Section 1 were employed. Then, immediately upon reaching isotope steady states in all compartments (i.e., after 30 min) we let k_{12}, k_{21}, k_{13}, k_{31}, and k_{75} be zero (simulating Zerahn's wash-out conditions), thereby entering into the "decay phase" in which certain fluxes ($k \times S$), namely entry of sodium from the epidermal side (1) and return of sodium from the corium side (7) into the epidermis was instantaneously abolished. For convenience in programming the appropriate k, rather than the associated S values were set at zero. Decay rates were obtained for all individual internal Na* pools of the model (S_2^*, S_3^*, S_4^*, S_5^*), and for the combined pools, $\Sigma S_2^*\, S_3^*\, S_4^*\, S_5^* = \Sigma S_j^*$. In addition, data were obtained on the rate of Na* accumulation in the external compartment 7.

5. Protocols and Data Derived by Calculations

For two models, abbreviated sample protocols are given in Table 1 to explain the calculations performed, using the original "print-out" results as they appeared on the computer data flow sheets (line a, Table 1). The data in lines b and c are in accordance with the definitions given in Section 2. The subscripts n and i indicate the type of study, net flux in 10Ec, and influx in W10E. S_{jn} is the Na^+ pool under steady-state net flux conditions. $P_n = \Sigma S_{jn}$ (total Na^+ pool), and $P_i^* = \Sigma S_{ji}^*$, the combined effective Na* pool under influx conditions. From this the percent distribution of sodium in the compartments was calculated (line h). Values for $[Na^+]_j$ (line f) were obtained from S_{jn} and the assumed (constant) volumes of the compartments (*see* Fig. 1 of ref. [7]). $V_{23}(\phi_3 - \phi_2)$ (line g) was calculated by the Nernst equation assuming Na^+ permselectivity of the barrier between compartments 2 and 3 [9]. Transmembrane flux rates (lines d and e; no example for J_b is

Table 1. Abbreviated sample protocols for models 10Ec and W10E

Pools	Model 10Ec, Net flux[a]						Model W10E, Influx[b]		
	S_{2n}	S_{3n}	S_{4n}	S_{5n}	P_n	S_{7n}	S^*_{5i}	P^*_i	S^*_{7i}
a) Print-out	0.010275	0.0029170	0.488320	0.062499	0.56401	575.0488	0.0052791	0.038742	0.59750
b) μEquiv Na^+	0.010275	0.0029170	0.488320	0.062499	0.56401	575.0488			
c) $\times 10^8$, cpm Na*							0.52791×10^6		59.75×10^6
d) J_i, μEquiv $\times$ $cm^{-2} \times hr^{-1}$								1.238	
e) J_n, μEquiv $\times$ $cm^{-2} \times hr^{-1}$				1.184					
f) [Na^+], mM	102.8	5.83	122.1	125.0		115.0098			
g) V_{23}, mV	+72.3	+72.3							
h) Na distribution (%)	1.82	0.52	86.6	11.1	100.0		13.6	100.0	

The numbers in line a) give the raw data as read from the computer flow sheets 30 min after starting the run. The data in lines b) and c) express the chemical meaning given to the print-out numbers. Lines d) through h) show values for derived data, calculated by using the characteristic parameters for these models as stated in sections 1 and 5 of the text.

[a] At zero time $S_1 = S_7 = 575.0000$; all other compartments empty.

[b] At zero time all compartments (1–7) are thought to be in steady-state Na^+ equilibrium for the condition $S_1 = S_7 = 575.00$ when Na* is added to compartment 1 to give 575×10^8 cpm. Specific activity $\sigma_1 = 1.000 \times 10^8$ cpm/μEquiv Na^+.

Table 2. Na^+ distribution and Na^+ pool fractions in compartments 2, 3, 4 and 5 under steady-state influx, backflux and net flux conditions; steady-state $[Na^+]$ in these compartments, and electrical potential V_{23}; steady-state transmembrane flux rates under influx, backflux, net flux conditions

Compartment	10Ed Weak pump only		10Ec Strong pump only		10E Weak & strong pump	
	Na^+ distribution (%)	Effective Na^+ pool fraction (%)	Na^+ distribution (%)	Effective Na^+ pool fraction (%)	Na^+ distribution (%)	Effective Na^+ pool fraction (%)
Influx						
a) 2	17.4	97.5	17.4	99.8	26.5	99.9
b) 3	66.1	76.5	3.7	73.8	5.5	76.5
c) 4	14.2	3.9	70.0	8.5	54.4	8.5
d) 5	2.3	2.5	8.9	8.4	13.6	8.4
e) P_i	0.063985 μEquiv		0.059026 μEquiv		0.038729 μEquiv	
Backflux						
f) 2	0.1	2.6	0.003	0.2	0.005	0.2
g) 3	4.4	23.5	0.2	26.2	0.2	23.6
h) 4	76.3	96.1	88.5	91.5	79.7	91.5
i) 5	19.2	97.5	11.3	91.6	20.1	91.6
j) P_b	0.293213 μEquiv		0.504989 μEquiv		0.285320 μEquiv	
Net flux						
k) 2	3.2	100.0	1.8	100.0	3.2	100.0
l) 3	15.5	100.0	0.5	100.0	0.9	100.0
m) 4	65.1	100.0	86.6	100.0	76.6	100.0
n) 5	16.2	100.0	11.1	100.0	19.3	100.0
o) P_n	0.357202 μEquiv		0.564011 μEquiv		0.324050 μEquiv	
$[Na^+]$ mM						
p) 2		114.5		102.8		102.7
q) 3		110.7		5.8		5.6
r) 4		58.2		122.1		62.1
s) 5		115.3		125.0		125.3
Fluxes, μEquiv × cm^{-2} × hr^{-1}; Electrical potentials, mV						
t) J_i		0.340		1.201		1.237
u) J_b		0.293		0.017		0.015
v) J_n		0.047		1.184		1.222
w) V_{23}		+0.9		+72.3		+73.3

included) were calculated in two ways with identical results. First, by reading from the print-out data sheet the increment in print-out numbers (i.e. μEquiv Na^+) for a given time interval after the system had reached steady state; second, by applying the integrated steady-state flux equations

for the time from 30 to 90 min which are for influx [Eq. (1)] and backflux [Eq. (2)]:

$$S_{7(30)} = \frac{k_{57}}{k_{75}} S_{5(30)} - \frac{k_{57}}{k_{75}} S_{5(30)} e^{-60k_{75}} + S_{7(30)} e^{-60k_{75}} \tag{1}$$

$$S_{1(90)} = \frac{k_{21} S_{2(30)} + k_{31} S_{3(30)}}{k_{12} + k_{13}} - \frac{k_{21} S_{2(30)} + k_{31} S_{3(30)}}{k_{12} + k_{13}} e^{-60(k_{12}+k_{13})} + S_{1(30)} e^{-60(k_{12}+k_{13})}. \tag{2}$$

It has previously been shown [7] that in steady-state influx and backflux only certain fractions of the sodium pools of the individual compartments, as obtained under net flux conditions, are effectively involved in unidirectional transmembrane fluxes. These fractions are calculated as, e.g., $100 \times S_{2i}/S_{2n}$, or $100 \times S_{3b}/S_{3n}$. Table 2 gives examples for effective Na^+ pool fractions.

Mention should also be made of the results on checking the steady-state condition $dS_j/dt = 0$ in all internal compartments, and for all variations of models used here. The appropriate differential equations are given in a previous paper [7]. The zero condition was fulfilled to the degree that values of the order 10^{-5} to 10^{-7} were obtained in all but two cases (10Ec backflux and net flux) where dS_4/dt gave values of 10^{-3} and 10^{-4}.

6. Results

(a) Strong and Weak Na^+ Pump Characteristics

The main reason for presenting the data given in Table 2 is to describe the characteristic functions of the "strong" and "weak" Na^+ pumps in model membrane 10E. The two Na^+ pump steps are: between compartment $3 \rightarrow 5$ ($k_{35} = 10$; $k_{53} = 0.1$; strong pump), and between compartments $4 \rightarrow 5$ ($k_{45} = 0.5$; $k_{54} = 2.0$; weak pump). We were now interested in knowing what contribution the weak pump makes to the net transmembrane Na^+ flux. Therefore, one or the other pump was taken out of action. When $k_{45} = 0.25$ and $k_{54} = 2.0$ (leaving k_{35} and k_{53} as stated) the weak pump effect is abolished (10Ec), as explained in Section 1. When k_{35} and $k_{53} = 0.1$ (leaving k_{45} and k_{54} as in 10E), the strong pump effect is abolished. The results of the computer runs with interpretations and calculations as explained earlier are shown in Table 2. Some of the data are given for the sake of completeness of the records and are of interest in connection with our previous publication [7]. In the context of the present study, attention is called to the results listed in lines p through w. With only the weak pump

in operation (10Ed), $[Na^+]_4$ (remaining cell $[Na^+]$) is relatively low, while $[Na^+]_3$ (1.RCL$[Na^+]$) is high, as is $[Na^+]_2$ ($[Na^+]$ in the subcorneal space the pre-Na^+ transport compartment). The reverse is the case when only the strong pump is in operation (10Ec). $[Na^+]_5$ ($[Na^+]$ in the extracellular space) is very slightly above $[Na^+]$ in the external fluid compartments, (1, and 7) when only the weak pump is functioning; but $[Na^+]_5$ is significantly higher than the $[Na^+]$ in the external compartments when only the strong pump operates. The main difference between 10Ec and 10E (with both pumps in action) is that $[Na^+]_4$ is kept relatively low. Inspection of the flux data in Table 2 shows that the weak pump makes only a very small contribution to the net transmembrane Na^+ flux. One may question whether the value $[Na^+]_4 = 122.1$ mM, in the absence of the weak pump, is reasonable, physiologically speaking. This question cannot be answered at this time. It can be pointed out, however, that these results of model experimentations are in line with the conclusions drawn many years ago from laboratory work [6], namely, that there seems to be compartmentalized functions in the handling of the Na^+ metabolism in frog skin epidermis: One concerned with "maintenance electrolyte equilibrium", reflected in the behavior of compartment 4 of the model; another with "unidirectional active ion transport", reflected in the behavior of compartment 3 of the model. In brief, the weak pump acts mainly as an internal maintenance pump, the strong pump as a transmembrane flow pump.

(b) Reaching Steady States during Na Influx (Loading Phase)*

The kinetics of loading with Na*, and of wash-out (decay) of Na* from the multicompartmental system shown in Fig. 1 of ref. [7] was studied under two conditions: With both Na^+ pumps in operation (W10E), and in the absence of Na^+ pump actions (W13G). The W indicates that wash-out followed immediately after steady states were reached. The k-coefficients in W10E were the same as in 10E. The k-coefficients in W13G were also those used in 10E, except that $k_{35} = k_{53} = 0.1$; and $k_{45} = 0.25$ and $k_{54} = 2.0$ (*see* Section 6*a*). Complete suppression of the Na^+ pumps simulates the effect of ouabain on Na^+ transport across frog skin [8, 10, 12]. Fig. 1*A* and *B* show the results obtained on loading of 10WE and WG13, respectively. Very near steady states were reached in all internal compartments (2, 3, 4, and 5) within 30 min. The sodium specific activity in compartment 1 (σ_1) remained nearly constant, as it should be, simulating actual laboratory experiments. Na* accumulated in compartment 7. When the data were plotted on ordinary graph paper, it was seen that after 10 min Na* accu-

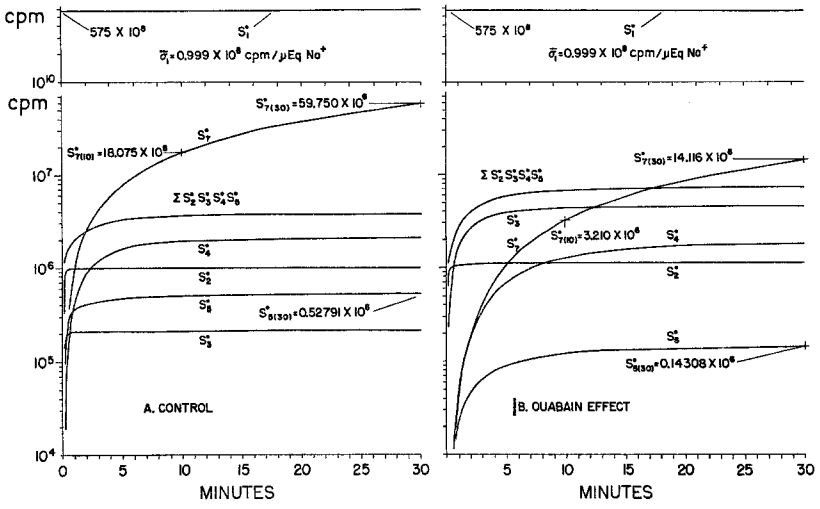

Fig. 1. (*A*) Kinetics of reaching steady-state conditions for influx of Na* in model W10E (with Na^+ pumps) and accumulation of Na* in external compartment 7. (*B*) The same for model W13G (no Na^+ pumps), simulating the ouabain effect in frog skin epidermis

mulated practically linearly with time. From the data in Fig. 1, or by applying Eq. (1), the rate of steady-state Na^+ influx (J_i) was calculated for W10E, $J_i = 1.237$ μEquiv × cm^{-2} × hr^{-1} (*see also* Tables 1 and 2). This flux rate is in agreement with laboratory experiments on isolated frog skin (*Rana temporaria*; *esculenta*; *pipiens*). For W13G, $J_i = 0.336$ μEquiv × cm^{-2} × hr^{-1}. It should be mentioned, that in the absence of all Na^+ pump activities, as in W13G, the rate of Na^+ backflux $J_b = J_i$, so that $J_n = 0$, whereas in the case with Na^+ pumps in operation (W10E), $J_b = 1.2\%$ of J_i [7]. The simulated flux data compare quite favorably with those reported by Nagel and Dörge [10]. Their J_i (μEquiv × cm^{-2} × hr^{-1}) values are as follows: Controls, 1.75 ± 0.14 (SEM, 13 experiments), ranging from 1.07 to 2.56; ouabain-treated skins, 0.26 ± 0.03, ranging from 0.16 to 0.50. Using the print-out data, obtained at 0.2-min intervals, as they appeared on the computer data flow sheets, and treating them in the manner as has been done by Hoshiko and Ussing in their laboratory studies [5], we have calculated values for the half time for the flux build-up. These authors have plotted $100\,(1 - m/M)$ *vs.* time in which m is the rate of appearance of Na* in the solution at the inside of the skin (compartment 7), and M is the final steady-state rate value. For W10E the value is 2.2 min for the time period from 1 to 10 min. This is in fair agreement with results by Hoshiko and Ussing; they give an average value of 3.4 min for skins in Cl^--Ringer's (*see* their Table 1). It

should be mentioned that in the time period from 0 to 1 min, a fast component, half time 0.16 min was noticed in the computer simulation studies. There are no experimental data available [5] for comparison. Cereijido and Rotunno [3] found a half time for flux build-up of about 7.5 min for skins of *Leptodactylus ocellatus* in sulfate-Ringer's. To obtain a value for the half time for flux build-up in W13G (simulating the actions of ouabain) an extrapolated value for M had to be obtained and was used. It was 0.576×10^6 cpm at $t = 50$ min. By using this, one obtains for $J_i = 0.345$ μEquiv $\times$ $cm^{-2} \times hr^{-1}$, which is only 2.7% greater than the J_i value already given above. Treating now the W13G data as those obtained in W10E, a value for the half time for flux build-up of 3.8 min was calculated for the period from 0 to 8 min. The process, however, is not a single exponential function. A slower component with half time of 6.0 min was seen for the period from 8 to 30 min. The increase in half time for flux build-up from 2.2 (W10E) to 3.8 to 6.0 min is in agreement with the measurements by Nagel and Dörge on skin (*R. esculenta*) [10]. They give average values (13 experiments, their Table 3) for $t_h = 3.19 \pm 0.29$ min for controls, and 8.10 ± 0.78 min for ouabain-treated skins. This effect of ouabain is also illustrated in Fig. 3 of the paper by Zerahn [12].

Comparing the 30-min values for $\Sigma S_2^* S_3^* S_4^* S_5^*$ in the models with, and without operation of Na^+ pumps (W10E; W13G), i.e. the Na* pool sizes P_i^* under identical conditions of loading with Na* from the outside (compartment 1), the following values were obtained: W10E, $P_i^* = 3.8742 \times 10^6$ cpm; W13G, $P_i^* = 7.2712 \times 10^6$ cpm, a nearly twofold increase in P_i^* under "ouabain conditions". This result fits in between the observations made on skin by Zerahn [12], who found a two- to sixfold increase, and those made by Nagel and Dörge [10], and by Aceves and Erlij [1] (on isolated epidermis), who found no increase in ouabain-treated preparations applying Na* from the outside.

(c) Na Wash-out Kinetics (Decay Phase)*

When models W10E and W13G were very nearly in Na* steady state, i.e. after 30 min, the decay phase began without delay. The first print-out number appeared after 0.2 min. The results are shown in Fig. 2*A* and *B*. In W10E, S_2^* and S_3^* decayed very rapidly and in a more complex fashion when compared to S_4^*, S_5^*, and $\Sigma S_2^* S_3^* S_4^* S_5^*$. Fig. 3 shows the fractions of Na* remaining in the compartments for a 10-min decay period. Maximal pool activity obtained in the 30-min loading period was set equal to 100. At time 45 min (i.e. 15 min after decay was begun), S_j^* in all compartments decayed at nearly the same rate. Table 3 gives values for decay coefficients

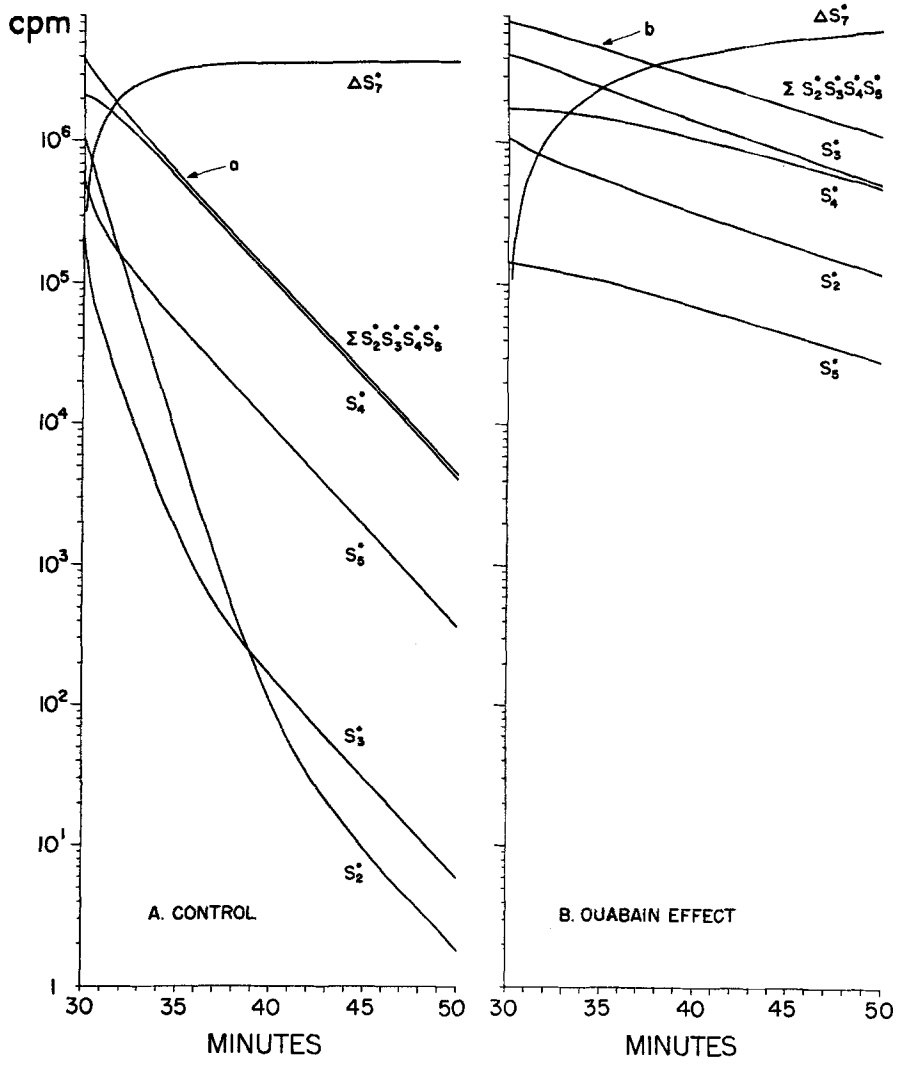

Fig. 2. (*A*) Kinetics of the Na* wash-out process in model W10E (with Na^+ pumps). Wash-out started at $t=30$ min, after preloading with Na* had led to near steady-state conditions in all internal compartments. ΔS_7=increment of Na* accumulation in external compartment 7 during the wash-out phase. (*B*) The same for model W31G (no Na^+ pumps)

($\alpha-\varepsilon$), and half times (t_h) for the decay processes. They were calculated by Eqs. (3) and (4); e.g. for α:

$$\alpha=\frac{\log_{10} S^*_{j(t_2)}-\log_{10} S^*_{j(t_1)}}{0.4343\,(t_2-t_1)} \tag{3}$$

$$t_h=\frac{0.6931}{\alpha}. \tag{4}$$

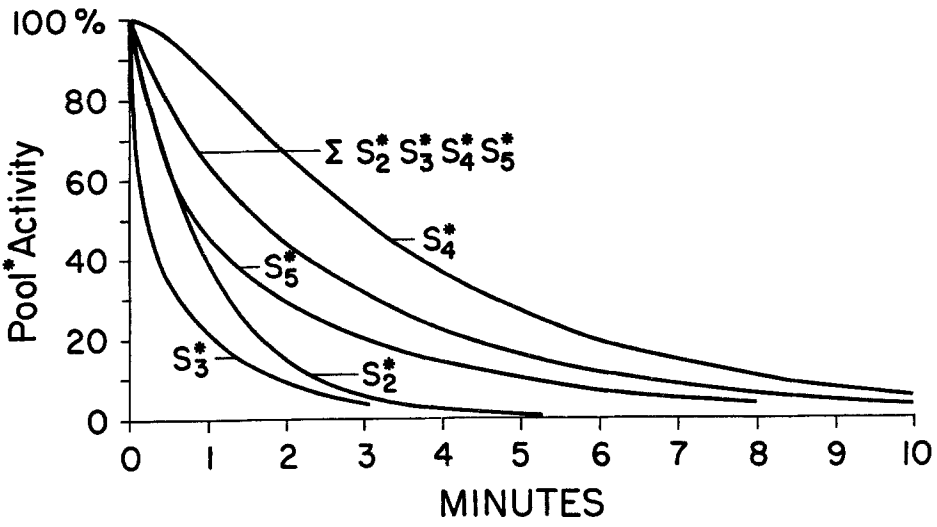

Fig. 3. Percent Na* pool activity remaining in the internal compartments during the first 10-min wash-out period. At the beginning, S_5^* follows the curve S_2^*

Table 3. Summary of data on decay coefficients, min^{-1} and half times, $\text{min}\,(t_h)$ calculated from computer studies of Na* washout in various models

Model	Compartment				
	2	3	4	5	Σ2, 3, 4, 5
	Decay coeff. α	Decay coeff. β	Decay coeff. γ	Decay coeff. δ	Decay coeff. ε
Model W10E (control), no delay time					
a) 32 to 50 min					0.326 (t_h=2.13) [a]
b) 45 to 50 min	0.333	0.326	0.327	0.327	0.327
Models W10E(6) – W10E(9), with delay time					
c) 34 to 50 min					0.327 (t_h=2.12)
Model W13G (ouabain effect), no delay time					
d) 30 to 50 min					0.093 (t_h=7.45) [a]
e) 45 to 50 min	0.106	0.106	0.090	0.095	0.093

[a] Data obtained by Zerahn (his Fig. 2) are as follows: ε=0.26 min^{-1}, t_h=2.7 min in control skin; ε=0.026 min^{-1}, t_h=26.7 min in ouabain-treated skin. Nagel and Dörge give the following values (averages of 7 experiments): ε=0.239 min^{-1}, t_h=2.90 min in control skin; ε=0.085 min^{-1}, t_h=8.2 min in ouabain-treated skin.

ΔS_7^* gives the amount of Na* accumulated above $S_{7(30)}^*$. It can be seen that at time 45 min (i.e., 15-min wash-out period) nearly all Na* was lost from the model membrane. When the Na^+ pumps were taken out of action

(simulating the ouabain effect) the rates for wash-out of S_j^* in all compartments were greatly reduced (Table 3).

We thought it of particular interest to further analyze the decay processes looking at $\Sigma S_2^* S_3^* S_4^* S_5^*$. It is these graphs, Fig. 2*A* and *B*, lines *a* and *b*, that must be compared with actual laboratory experiments [10, 12]. From the information given in Table 3 it can be concluded that there is very good agreement in the kinetic data obtained by the models W10E and W13G, and the laboratory data provided by Zerahn [12] and by Nagel and Dörge [10]. The t_h value in ouabain-treated skins given by Zerahn [12] is approximately 3 times greater than that found by Nagel and Dörge [10]. It must be pointed out, however, that the experimental conditions in the studies by Nagel and Dörge [10] differed from those used by Zerahn [12] in several respects. 1) Na*-loaded skins were "open" in both directions during wash-out, towards the outside and the inside fluid compartment. 2) The skins were kept short-circuited during the wash-out phase; this was not the case in Zerahn's experiments. 3) The inside and outside fluid compartments had a volume of 0.6 ml and solutions flowed past both membrane surfaces at the rate of 4 to 6 ml/min. In Zerahn's work no outside fluid was present during the wash-out phase, and the volume of the inside solution was made in excess of 500 ml. We have modeled only Zerahn's experiments, favoring his experimental set-up. Nevertheless the t_h values in the controls under either conditions are nearly identical. The differences observed under ouabain conditions may be the result of differences in the methodology and scarcity of data with statistical information.

Focusing attention again on line "*a*" (Fig. 2*A*), and considering it as a laboratory wash-out result, justification for which is provided by the data in Table 3, one is, of course, tempted to resolve this nonlinear event into linear components by the widely used procedure described in detail by Defares and Sneddon [4]. This is shown in Fig. 4. It was impossible to split up line "*a*" into more than two straight lines, although there is a nonlinearity barely noticeable in region *B* in Fig. 4. From this one would be led to the false conclusion, that line "*a*" is, essentially, made of two rate processes, given by the second-order equation:

$$(\text{cpm})_t = 0.677 \times 10^6 \, e^{-0.98644t} + 3.05 \times 10^6 \, e^{-0.32607t}. \tag{5}$$

The points indicated on line "*a*" are the values calculated by this equation. Since it is known from the design of the model (*see* Fig. 1 of ref. [7]) that there are four membrane compartments involved which produce the decay curve, line "*a*", one can write an equation for this curve also as

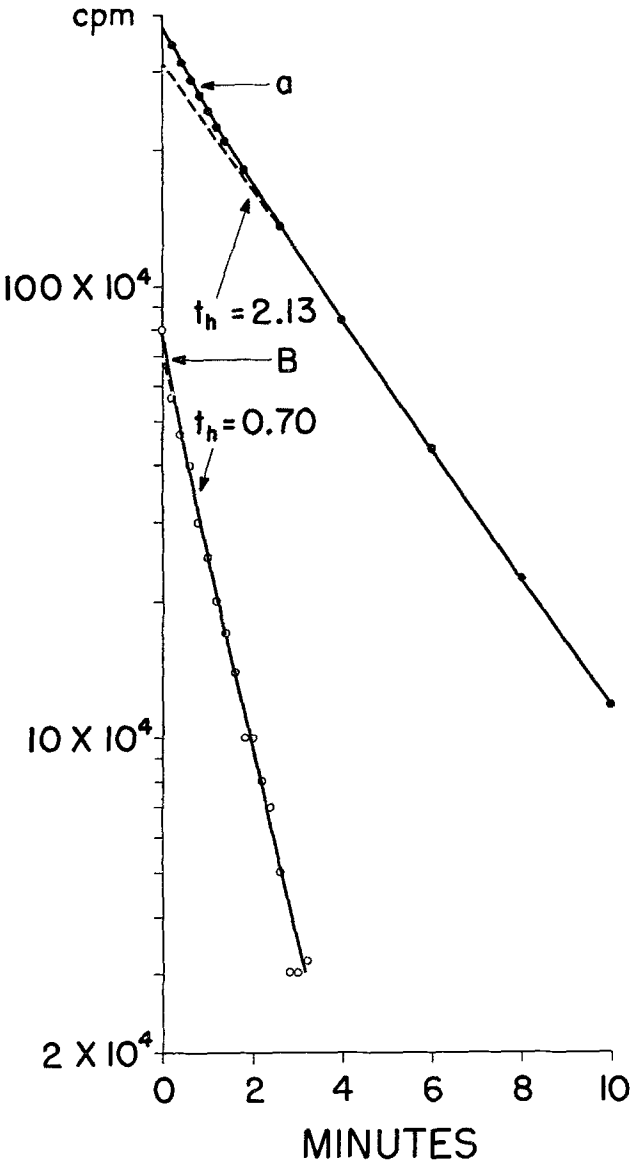

Fig. 4. Result of splitting decay curve "a" ($\Sigma S_2^* S_3^* S_4^* S_5^*$) into linear components. Line "a" is the same as the one shown in Fig. 2*A*. At *B*, a nonlinearity is just noticeable, but the graphic method fails to resolve this early event

follows:

$$(\text{cpm})_t = 1\times10^6 e^{-0.94t} + 0.15\times10^6 e^{-0.78t} + 2.5\times10^6 e^{-0.32t} + 0.4\times10^6 e^{-0.36t}. \quad (6)$$

The parameters in this equation were obtained by drawing best fitting straight lines (by inspection) through the decay curves for S_j^* in compartments 2 (first term), 3, 4, and 5 (last term). The values calculated from

Eq. (6) fall very nearly on line "a". Obviously, this equation is not entirely correct, but taken as an approximation, it shows at least participation of all membrane compartments. Our intent, here, is to emphasize that, given an experimental curve like line "a", the described and often used method of analysis is not sensitive enough when applied to the epidermis of frog skin; there is little hope to identify the nature of all compartments, especially the important Na^+ transport compartment [No. 3, Fig. 1 (of ref. [7]) according to our assumption]. Even in a computer simulation study, where it is possible to investigate the events during the first two minutes of the wash-out phase with great precision, one cannot obtain a value for S_3^* (Na* pool in the transport compartment) by the method of splitting the $\Sigma S_2^*\ S_3^*\ S_4^*\ S_5^*$ decay curve. From the model data presented in Fig. 2A it should be feasible, however, to obtain in laboratory studies on frog skin values for $(S_2^* + S_3^*)$ and $(S_4^* + S_5^*)$. This will be discussed in Section 7.

(d) Significance of Delay Time

An additional aggravating situation can arise in laboratory studies on the wash-out kinetics because of an unavoidable lag in time (delay time) between termination of loading to reach steady state, and the beginning of collection of decay data. In practice this has amounted to approximately 2 min [2, 12]. During this time, when the supply of Na* from the external compartment is cut off, there must occur a considerable redistribution of Na* in the internal membrane compartments. We have studied this redistribution on model W10E (both Na^+ pumps in operation). The results are given in Table 4. When steady state was reached, 32% of the Na* is found in compartments 2 and 3, and 68% is present in compartments 4 and 5. Two minutes later, when the wash-out process is under way, but data on Na* in the internal compartments (the skin) are not yet obtained, only 9.6% of the total Na* is located in (2+3), and 90.4% is present in (4+5). We have pointed out in Section 6a that the weak or maintenance pump (4→5) contributes only insignificantly to the transmembrane Na^+ flux. Therefore 90.4% of the Na* in the membrane that is washed out is Na* that "behaves as if it has passed the transporting mechanism" [12]. Inspection of the decay curves for S_4^* and S_5^*, Fig. 2A, shows that the decay rate coefficients for the period from 32 to 50 min are identical, and they are also equal to the decay rate coefficient, for $\Sigma S_2^*\ S_3^*\ S_4^*\ S_5^*$. The values are given in Table 3 ($\gamma = \delta = \varepsilon = 0.327\ \text{min}^{-1}$). These findings obtained on the model membrane as shown in Fig. 1 of ref. [7] and with specifications as selected for model W10E, are in very good agreement with Zerahn's data on skin, and his conclusions. According to the model data (Table 4) there

Table 4. Effect of delay time on distribution of Na* in the pretransport and transport compartments (2+3), and remaining cell and extracellular space compartments (4+5) of Model W10E

S_j^*	Delay time (min)					
	0[a]		1.0[b]		2.0[c]	
	cpm $\times 10^{-6}$	%	cpm $\times 10^{-6}$	%	cpm $\times 10^{-6}$	%
$\Sigma S_2^* S_3^* S_4^* S_5^*$	3.874260	100.0	2.477158	100.0	1.704461	100.0
S_2^*	1.025800		0.386960		0.145800	
S_3^*	0.214350		0.045168		0.018001	
$\Sigma S_2^* S_3$	1.240150	32.0	0.432128	17.4	0.163801	9.6
S_4^*	2.106200		1.803300		1.386900	
S_5^*	0.527910		0.241730		0.153760	
$\Sigma S_4^* S_5$	2.634110	68.0	2.045030	82.6	1.540660	90.4

[a] Steady-state loading values at time 30 min, $S_{j(30)}^*$.
[b] Values at time 31 min, $S_{j(31)}^*$.
[c] Values at time 32 min, $S_{j(32)}^*$.

should be a fraction of Na*, 9.6%, that has not yet passed the transporting mechanism, and it should be detectable even with delay of 2 min before commencing with obtaining wash-out data. It would seem, however, that to measure this fraction, a considerable number of experiments must be carried out for statistical calculations. It must also be said that all results obtained with model W10E depend on the correctness of the assumed volumes of the components of the system. Especially critical here, is the assumption that the volume of compartment 2 (subcorneal space) is 0.1 μliter/cm^2. The size of this space has never been measured. If this is an overestimation, the $\Sigma S_2^* S_3^*$ figure would be smaller than given in Table 4. This would further reduce any chance to measure anything else but S_4^* and S_5^*, i.e. Na* in the remaining cell compartment (with maintenance Na^+ pumps only), and in the extracellular space.

The preceeding applies to delay which occurs before the first decay result is recorded, while Na* flows into the internal compartment 7 upon cutting off the supply of Na* from external compartment 1. In the computer simulation studies, this was accomplished by making k_{75} (as well as $k_{12}, k_{21}, k_{13}, k_{31}) = 0$, but keeping $k_{57} = 4\ \text{min}^{-1}$ (Section 1). This is equivalent to saying that the volume of compartment 7 instantaneously becomes very large. In practice this maneuver will take some time, and we were, therefore, interested in finding out how this delay time will affect the distribution of Na* in model W10E. This was done by making and keeping not only $k_{75} = 0$, but k_{57} as well, but the latter only for a short period of

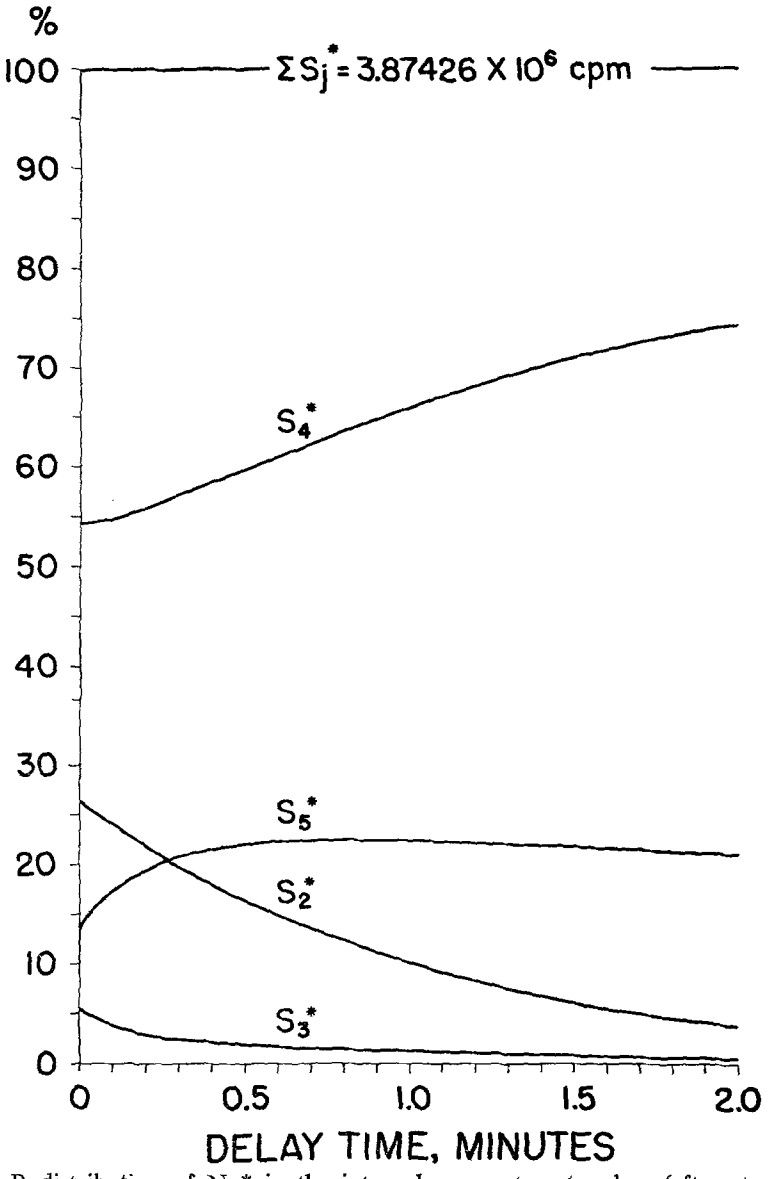

Fig. 5. Redistribution of Na* in the internal compartments when (after steady-state loading) Na* is prevented from entering external compartment 7 for a period of maximally 2 min

time. The result on Na* redistribution is shown in Fig. 5, and the corresponding wash-out curves for ΣS_2^* S_3^* S_4^* S_5^* are presented in Fig. 6. It can be seen that the effect of delay time is such that it obscures the realization of $(S_2^* + S_3^*)$. Na* is rapidly shifted from compartments 2 and 3 into compartments 4 and 5. Preventing flow from $5 \rightarrow 7$ for 2 min leads to redistribution of Na* such that $(S_2^* + S_3^*)$ is only 4.5% of the total Na* present, an

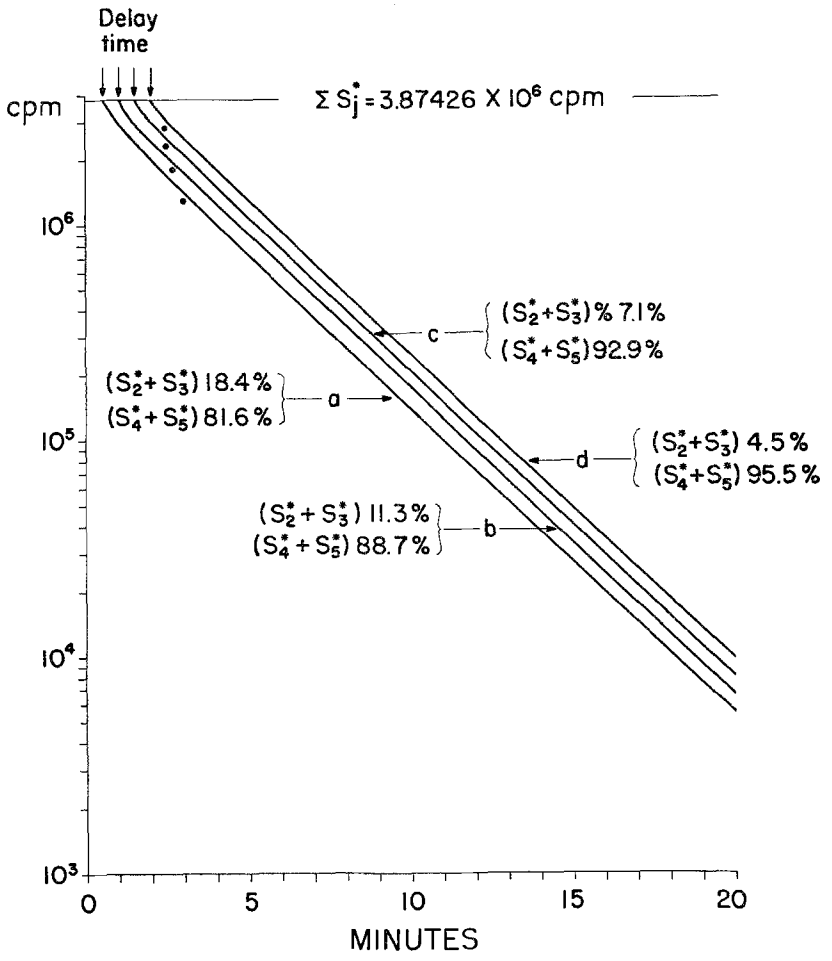

Fig. 6. Effects of delayed escape of Na* from the preloaded model membrane into external compartment 7. Decay is shown for $\Sigma S_2^* S_3^* S_4^* S_5^*$. The dots near the curves (upper left corner) indicate where the downward linearity of the decay process begins. The delay times were: 0.5 min (curve *a*); 1.0 min (curve *b*); 1.5 min (curve *c*); 2.0 min (curve *d*). During these times internal redistribution of Na* had occurred, as shown in the illustration. The figures are those obtained from data given in Fig. 5

amount which would be difficult to measure. The dots near the curves indicate where (seen better on large graphs) the nonlinear components, attributable to S_2^* and S_3^*, begin to become evident. The greater the delay time the less these pools become apparent, in agreement with the redistribution data given in the graph.

7. Discussion

Much of the discussion has already been presented in Section 6 for the reason of maintaining a better continuity of the text, where it was of interest

to compare the computer simulation data with laboratory results. From the material presented it is concluded that studies on the kinetics of wash-out of Na* from preloaded skins are not likely to give an estimate of the active transport pool which seems to be located near the outer surface of the epidermis. We have assumed that its location is in the 1.RCL (compartment 3 in Fig. 1 of ref. [7]). However, under certain circumstances one may be able to obtain an estimate of the Na* present in the subcorneal space (pretransport compartment) and the transport compartment, $S_2^* + S_3^*$. Fig. 1*A* shows that the rates of wash-out for pools S_2^* and S_3^* are considerably greater than the rates of wash-out for pools S_4^* and S_5^*; i.e., Na* in the remaining cell compartment and in the extracellular space. Eq. (6) describes very nearly correctly the kinetics of total washout curve

$$(\Sigma S_2^*\ S_3^*\ S_4^*\ S_5^* = \Sigma S_j^*),$$

the curve that is in good agreement with laboratory observations (Section 6*c*). This is for the wash-out period from 0 to 30 min. For the first 10 min the rate of loss of Na* from compartments 2 + 3 follows very closely the equation:

$$(\text{cpm})_t = 1.03 \times 10^6\, e^{-0.975t} + 0.21 \times 10^6\, e^{-0.975t}$$

or

$$(\text{cpm})_t = 1.24 \times 10^6\, e^{-0.975t}. \tag{7}$$

When Eq. (7) is compared with Eq. (5) it is seen that Eq. (5), which is obtained by the method of splitting the ΣS_j^* wash-out curve (Fig. 4) gives very nearly half of the Na* pool in compartments 2 and 3, which is the Na* awaiting transport. This is the best estimate that could be made from studies on the kinetics of the Na* wash-out process. The reason why the pools $(S_2^* + S_3^*)$ are underestimated will become apparent if one observes the fact, shown in Fig. 4, that there is in region *B* a nonlinearity which, however, cannot be resolved. Thus, the difficulty with this method of estimating the pool of Na* awaiting transport is obvious. Nevertheless, it should be possible to obtain useful data, especially when aiming only at observations on relative changes in pool size under varying experimental conditions. Careful consideration must be given to the delay time which occurs when switching from the loading phase to the decay phase because of rapid redistribution of Na* within the epidermis during this period of time (Section 6*d*). An additional complication is seen in the fact that the epithelium of the skin glands may participate in the loading as well as in the wash-out process. These conclusions are based on the assumption that the model shown in Fig. 1 (ref. [7]), with specifications as given for W10E, bears close resemblance to the structure and function of frog skin epidermis.

Evidence for this is found in the present paper (Table 2) as well as in a previous publication [7]. In the earlier study (*see also* Table 2 of the present paper) it was found that model 10E is similar to frog skin epidermis with respect to (a) rates of transepithelial influx, outflux and net Na^+ flux ($1.2\ \mu Equiv \times cm^{-2} \times hr^{-1}$); (b) steady-state time (15 to 20 min); (c) pool fractions for Na^+ exchangeable from the epidermal, and the corium side of the skin (12 and 88%, respectively); (d) initial rate of Na* uptake, excluding glandular tissue (greater than transepithelial steady-state net flux rate; factor of <2); (e) changes in flux rates and pool sizes upon changing values of rate coefficients (simulation of ouabain, ADH, amiloride, catecholamine effects on skin); and (f) electrical potential at the "outer border" of skin epidermis, as measured by microelectrode puncture of the outermost cell layer (73 mV, 1.RCL+). Model 10E responds to changes in $[Na^+]_0$ with typical saturation effect on net Na^+ flux, and p.d. change (40 mV/decade change in $[Na^+]_0$; *see* preceding paper).

This work was supported by NIH Grant GM-03545-19.

References

1. Aceves, J., Erlij, D. 1971. Sodium transport across the isolated epithelium of the frog skin. *J. Physiol.* **212**:195
2. Andersen, B., Zerahn, K. 1963. Method for non-destructive determination of the sodium transport pool in frog skin with radiosodium. *Acta Physiol. Scand.* **59**:319
3. Cereijido, M., Rotunno, C. A. 1967. Transport and distribution of sodium across frog skin. *J. Physiol.* **190**:481
4. Defares, J. G., Sneddon, I. N. 1961. The Mathematics of Medicine and Biology, pp. 583–586. Year Book Medical Publishers, Inc., Chicago, Illinois
5. Hoshiko, T., Ussing, H. H. 1960. The kinetics of Na^{24} flux across amphibian skin and bladder. *Acta Physiol. Scand.* **49**:74
6. Huf, E. G., Doss, N. S., Wills, J. P. 1957. Effects of metabolic inhibitors and drugs on ion transport and oxygen consumption in isolated frog skin. *J. Gen. Physiol.* **41**:397
7. Huf, E. G., Howell, J. R. 1974. Computer simulation of sodium fluxes in frog skin epidermis. *J. Membrane Biol.* **15**:47
8. Koefoed-Johnsen, V. 1957. The effect of *g*-strophanthin (ouabain) on the active transport of sodium through the isolated frog skin. *Acta Physiol. Scand.* **42** (Suppl. 145):87
9. Koefoed-Johnsen, V., Ussing, H. H. 1958. Nature of the frog skin potential. *Acta Physiol. Scand.* **42**:298
10. Nagel, W., Dörge, A. 1971. A study of the different sodium compartments and the transepithelial sodium fluxes of the frog skin with the use of ouabain. *Pflüg. Arch. Ges. Physiol.* **324**:267
11. Smith, T. C., Martin, J. H., Huf, E. G. 1973. Sodium pool and sodium concentration in epidermis of frog skin. *Biochim. Biophys. Acta* **291**:465
12. Zerahn, K. 1969. Nature and localization of the sodium pool during active transport in the isolated frog skin. *Acta Physiol. Scand.* **77**:272